Achieving User-Level Fairness in Open-Access Femtocell based Architecture

Zhixue Lu Tarun Bansal Prasun Sinha
The Ohio State University
{luz, bansal, prasun}@cse.ohio-state.edu

Abstract

Femtocell based architectures have the potential to position the cellular service providers to compete head-on with the WiFi market. However, significant interference can happen due to unplanned deployments. Current use of hard partitioning approaches for resource allocation, and lack of guidelines for configuring the femtocells, make it difficult to obtain significant performance gains over traditional cellular networks. In this paper, we study the dynamic OFDMA sub-channel assignment problem while jointly considering power assignment and association control to provide $maxmin$ fairness. Towards this objective, we first consider a non-interfering model, which disallows interfering femtocells in the solution. A more general interfering model is then considered under which the problem is transformed into the *partition coloring* problem. We then show the NP-hardness of the problems and design centralized approximation algorithms with provable bounds and distributed solutions. Through extensive simulations in realistic settings we show that, compared to previous work, our solutions under the non-interfering model can achieve 2x of the minimum throughput, and under the interfering model the minimum throughput can be up to 3x of the baseline algorithms.

Index Terms

Femtocell, Fairness, Resource Allocation.

Achieving User-Level Fairness in Open-Access Femtocell based Architecture

I. Background and Motivation

Cellular network users have always been missing out on the broadband experience. Although new and upcoming cellular technologies such as OFDMA based WiMAX [1], [16], and LTE [2], [39], can provide data rates of several Mbps, that is still at least an order lower than the data rates supported by current WiFi technologies. This gap is fundamental and is expected to remain due to the difference in coverage range of cellular and wireless local area technologies.

Prior approaches to provide a broadband experience include cost-prohibitive pico- or microcellular architectures [36], [53]; and opportunistic ad-hoc networking of mobile devices [34]. More recently, a promising approach based on femtocells [9], [42], [50] is being incorporated by WiMAX, LTE and CDMA communities to improve the cellular experience and provide high data rate coverage over short ranges. Femto Base Stations (FBS) are small in-home cellular base stations that interact with the cellular backbone network via the broadband Internet connection.

Femtocells were initially designed to provide improved indoor coverage for signal-starved customers. ATT's 3G Microcell [9], Verizon's network extender [50], and Sprint's Airave [42] are recent products based on the concept of femtocells. Recent launch of these products from major cellular service providers clearly shows market support for such concepts.

However, with proper configuration, the FBSs can also provide coverage over significantly larger *outdoor regions* while allowing service to *all* subscribers. Such an *extended femtocell based architecture* will be beneficial for all the three parties: end customers, due to improved link quality; FBS owners, due to the generated revenue from providing support to the service provider; and, the cellular service provider, due to spatial reuse of limited channel resources. *This extended architecture has the potential to position the cellular service providers to compete head-on with the WiFi market. Its ubiquity can be a significant advantage over the spotty broadband coverage offered by today's scattered WiFi hotspots.*

Cellular service providers usually set aside a fixed and arbitrarily chosen number of channels for use by its femto users, and do not provide any guidelines for configuring the transmission power of arbitrarily deployed FBSs. Such static solutions are neither scalable nor optimum for controlling the interference between multiple FBSs, and between FBSs and macro base-station (MBS). It can significantly decrease user throughput or result in unfairness. To achieve both high throughput and fairness among users, making dynamic decisions becomes critical. Toward this objective, this paper solves the dynamic power control, sub-channel assignment, and association problems.

In a recent work [54], the uplink interference problem in co-channel femto networks was studied, in which macrocell users are protected with a higher priority than femtocell users by a distributed power management framework. Instead of co-channel deployment, *this paper focuses on orthogonal assignment of time-frequency resources in OFDMA network*. In another work [43], the problem of static sub-channel allocation to the femtocells was studied, without considering the throughput of individual users. In contrast, *this paper investigates the sub-channel assignment problem considering fair allocation to each individual user, while also jointly considering power assignment and association.* Note that our work also differs from the previous works on fairness in WLANs [10], [26], [28], which either address fairness by solely performing association control [10], [26], or by controlling the contention behavior of nodes in the IEEE 802.11 MAC layer [28].

Our study considers two models in the solution. The non-interfering model (NINT model) assigns power levels to each FBS in such a way that the femtocells do not interfere with each other, allowing for independent scheduling of users within each femtocell. This model requires low coordination as the FBSs can operate independently for scheduling transmissions to their users. The more general interfering model (INT model) allows the femtocells to interfere but the sub-channel assignment disallows interfering links to simultaneously transmit in the same time slot and the same sub-channel. Although the level of coordination needed is higher in this model, better performance can be expected as it is a generalization of the NINT model. As the FBSs and the MBS can use the wired backbone for exchanging control messages, both models are feasible to implement in practice. The contributions of this paper are as follows:

- Under the NINT model, we propose a $max\{\beta, 1/N\}$ bounded centralized approximation algorithm and a distributed solution for the $maxmin$ throughput problem, where β is the fraction of users that are outside the coverage range of any femtocell, and N is the number of users.
- We show that throughput can be further improved by introducing the INT model, and reduce the problem to the *partition coloring problem* [25], for which approximation algorithms with *provable bounds* were not known thus far. We then develop both centralized algorithm and localized

implementation, bounded by $O(\Delta \log N)$ where Δ is the maximum inter-partition degree and N is the number of users.

- We evaluate the performance of these solutions with extensive simulations and compare with two baseline approaches. While the solutions under the NINT model achieve $2x$ of the minimum throughput, the solutions under the INT model achieve up to $3x$ of the minimum and average throughput, compared with DRA+ algorithm [43].

The rest of the paper is organized as follows. Section II gvies an overview of related work. Section III presents the problem. In Sections IV and V, we propose our solutions for resource allocation under both the non-interfering and the interfering model. Section VI evaluates the performance of the algorithms under both models by simulations. Our future work is presented in Section VII. Finally, Section VIII concludes the paper.

II. Related Work

Due to its significance, resource allocation algorithms in OFDMA networks have been studied in many prior works. [15], [22] try to maximize the aggregate throughput, while [56], [57] aim to minimize power consumption. However, none of them address the fairness issue. Proportional fairness is considered in [23], [37], [41]. Resource allocations in those works are formulated as convex optimization problems, the objectives of which are to maximize sum of user rate. Proportional fairness is assured by imposing a set of constraints, and power assignment is either considered as a constraint, or is evenly allocated among all channels. Unlike those works, this paper formulates the resource allocation problem using graph based approach.

Graph-based approaches such as [13] apply graph coloring technique to solve the fractional frequency assignment problem in OFDMA networks with homogeneous cell size, without considering heterogeneous cell size or fairness. [29] solves the subcarrier selection, transmission mode selection and relay selection problem for relay-assisted bidirectional OFDMA network, which is not suited for femtocell network. [55] develops optimal algorithms for resource allocation problem with user constraints. However, the objective of [55] is to maximize system throughput, which is essentially different from this work.

In the femtocell literature, femtocell solutions in the market are primarily UMTS and CDMA based, driven from a business perspective [18], that aim to improve indoor coverage using available backhaul (cable, DSL). However, as an emerging technology, the challenge of mitigating intra- and cross-tier interference is still critical in the current solutions [3], [12], [17]. Interference is usually addressed through power control [11], [14], [20]. [11] develops an uplink capacity analysis of a CDMA two-tier network. The authors show that interference avoidance can help achieve higher user capacity and avoid the design of protocols that require the mobile to sense the spectrum during handoff. [14] discusses some key requirements for co-channel operation of femtocells such as auto-configuration and public access, and proposes a power control method that ensures a constant femtocell radius in the downlink and a low pre-definable uplink performance impact to the macrocells. A simulation of femtocells deployed in a residential scenario is studied in [20], which shows that the deployment of these femtocells would not pose a significant impact on the dropped call rate of mobile users. The uplink interference problem in co-channel deployed femtocell networks is studied in [54], which presents a trifecta of distributed algorithms, mainly focusing on protection of macrocell users.

OFDMA-based femtocells have been gaining increased attention recently. In OFDMA based femtocell solutions, intelligent sub-channel allocation is an alternative to power adjustment to mitigate interference while improving the system capacity. A coverage and interference analysis based on a realistic OFDMA macro/femtocell scenario is provided in [31], and some guidelines on how the spectrum allocation and interference mitigation problems can be approached are further discussed. [7] carries out experimental studies to characterize interference in OFDMA femtocell network. [49], [51] study the open and close access problem for OFDMA femtocells, and suggest to use limited access mode [49] or to adapt access mechanism based on average cellular user density. Energy efficiency problem was recently studied in [27], [52], which aims to achieve energy efficiency at femtocells [52], and maximize the lifetime of handsets [27]. Self-organizing frameworks are studied in [4], [30]. [30] proposes a two-phase self-organizing framework to minimize interference and maximize network capacity, while [30] assumes femtocells and macrocell work on the same channel, and applies a non-cooperative game approach to maximize weighted sum rate. Neither of them addressed the fairness issue.

Resource allocation was recently studied in [6], [8], [19], [40], [43], [44]. [44] proposes an adaptive resource scheduling algorithm for wireless relay OFDMA networks. [6] designs and implemens an uplink scheduler for OFDMA femtocells, without considering downlinks. [40] introduces an interference avoidance framework by letting femtocells utilize resource blocks occupied by far away mobile stations, without considering the fairness issue. [19] proposes a cluster-based resource allocation scheme, which first builds clusters, and then preforms optimal resource allocation for each cluster. However, power adjustment is not considered in [19]. In [43], the authors propose a dynamic resource allocation mechanism between macro and femtocells to achieve proportional fairness among users. [8] proposes a femtocell resource management system that divides one OFDMA frame into two zones – the reuse zone and the isolation zone, which also categorizes users into two groups, correspondingly. Users in reuse zone will be simultaneously active, and deal with interference through link adaptation, while users in the isolation zone are isolated via resource allocation (based on weighted max-min fairness).

However, [43] and [8] only consider fixed power level and coarse resource allocation strategies (on per-femtocell basis) regardless of the possible variations of user density in different femtocells, all of which, in contrast, are considered in this work. Alternatively, this paper could serve as a complementary work for the resource isolation part of [8], when power adjustment or user density is available in the system.

III. Problem Statement

A. Notations

Consider a single macrocell base station (MBS) deployed in a 2D region that contains M FBSs $\mathcal{F} = \{f_1, \cdots f_M\}$. $\mathcal{U} = \{u_1 ... u_N\}$ is the set of N users in the system. The location of user u_i is given by $L(u_i) = (x(u_i), y(u_i))$. The location of FBS f_j is given by $L(f_j) = (x(f_j), y(f_j))$. Each FBS can operate at a power level chosen from the set $\mathcal{P}$ indexed by $\{1 \cdots l\}$, where the selected power for index k is given by $p(k)$, and $p(k) < p(k')$ for $k < k'$. For any FBS f_i associated with power level $p(k)$, we define the transmission range of f_i at power level $p(k)$ as the range within which the received signal strength from f_i is higher than some threshold RSS_{tx}. Formally, let r_k^{tx} denote this range, and $rss(f_i, k, d)$ denote the received signal strength at distance d from f_i sending beacons at power level $p(k)$, then $r_k^{tx} = \max\{d : rss(f_i, k, d) \geq RSS_{tx}\}$. Similarly, we define the interference range of f_i at power level $p(k)$ as the range within which a receiver associated with another FBS will receive an interference level from f_i that is higher than some other threshold RSS_{int} ($RSS_{int} \leq RSS_{tx}$), i.e., $r_k^{int} = \max\{d : rss(f_i, k, d) \geq RSS_{int}\}$. We assume that the MBS when transmitting interferes with all other nodes in the system. Let $\mu(j, l)$ be the number of users within the transmission range of FBS j when operating at power level l. To simplify the presentation, we assume that the interference range of all FBSs at their highest power levels are fully contained within the macrocell's boundary.

Let ρ_j be the power level selected by femtocell j. $\rho_j \in \mathcal{P} \cup \{0\}$, where $\rho_j = 0$ implies that FBS j is not active due to interference. The $N \times M$ matrix $\mathcal{B}$ represents the association of N users to the M femtocells. $\mathcal{B}_{ij} = 1$ if user i is associated with femtocell j, otherwise it is 0. Each user associates with at most one femtocell. Users not associated with any femtocell associate with the macrocell.

Consider an OFDMA frame as in Figure 1. Tiles are to be allocated in the system. Spatial reuse of the tiles is possible among FBSs. A fraction of time is allocated for uplink and another fraction for downlink communication. For simplicity, the discussion focuses only on the downlink, but the same framework can be applied to extend the solutions for uplink transmissions. Each downlink frame has t time-slots and c sub-channels. The tiles are further divided between the macrocell and the femtocells. A feasible allocation $\mathcal{A}$ is an assignment of a subset of links (FBS to user or MBS to user) to each tile, such that the links assigned to any given tile does not interfere with each other.

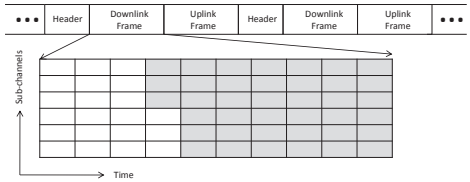

Fig. 1. OFDMA Frame Structure [43]: Gray tiles are for FBSs and the white for MBS. The header contains information on the allocation of the tiles.

B. Problem Statement

Our solution for resource allocation will determine multiple parameters: 1) the power level selected for each femtocell ($\vec{\rho}$); 2) the association of users to femtocells or the macro cell ($\mathcal{B}$); and, 3) assignment of tiles to the macrocell or multiple femtocells ($\mathcal{A}$). We focus on fair rate allocation among the users, and seek to compute the optimum $maxmin$ rate assignment problem.

IV. Resource Allocation with NonInterfering Femto-Cells

A. The NonInterfering Model

Under this model, the solution will ensure that the femtocells are not interfering when operating on the same channel by adjusting their power levels, i.e., there are no overlapping femtocells in the final solution. Thus under this model, all femtocells will be simultaneously active in all the tiles allocated to femtocells, and inactive in all the tiles allocated to the macrocell. So, all users in the same femtocell will have equal rate allocation (by round robin of the tiles allocated for femtocells), and similarly, users that are served by the macrocell will have equal rate allocation. Let τ_f be the fraction of tiles allocated to the FBSs, and $\tau_m = 1 - \tau_f$ be the fraction allocated to the macrocell. Under the constraint of non-interfering femtocells in the solution, without loss of generality, we consider the following objective function [1]:

$$\mathbf{P1} : \max_{\mathcal{B}, \vec{\rho}, \tau_f} \min_{1 \leq i \leq N} r_i \tag{1}$$

where r_i is the fraction of tiles allocated to user i from the downlink frame, which represents the effective data rate of user i.

Consider a user that is in range of an FBS in the final power allocation. If it associates with the MBS, then that slot will become busy for *all* FBSs. However, if it associates with that FBS, then other FBSs can also be active and reuse that slot (since all femtocells are non-overlapping in the solution). Thus associating with that FBS is the optimum decision. This implies that the association matrix $\mathcal{B}$ has been implicitly

[1] Alternatively, our solutions can be applied to the weighted version of $maxmin$ fairness problem

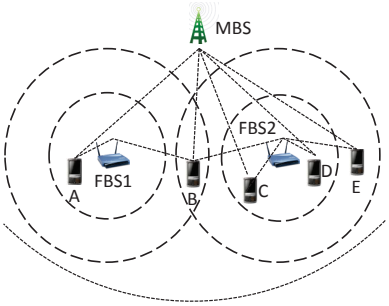

FBS1 power	FBS2 power	#Users (FBS1)	#Users (FBS2)	#Users (Macro)	Arg of Eq. 4	τ_m	τ_f	Throughput Vector (A,B,C,D,E)
Lo	Lo	1 (A)	2 (C,D)	2 (B,E)	3 – 2 = 1	1/2	1/2	1/2, 1/4, 1/4, 1/4, 1/4
Lo	Hi	1 (A)	4(B,C,D,E)	0	5 – 4 = 1	0	1	1, 1/4, 1/4, 1/4, 1/4
Hi	Lo	2 (A, B)	2 (C,D)	1 (E)	4 – 2 = 2	1/3	2/3	1/3, 1/3, 1/3, 1/3, 1/3
Hi	Hi	Not feasible in the non-interfering model						

Fig. 2. Resource Allocation: The dotted lines show the various possible communication ranges. The τ_m that determines the optimum $maxmin$ rate for the users is shown for each power combination. The (Hi,Lo) combination with a fractional allocation of 1/3 tiles for the MBS optimizes the objective.

solved: for users that are within the range of some FBS, they will associate with the corresponding FBS, otherwise, associate with the MBS. So, $P1$ could be simplified to the following without loss of generality:

$$\max_{\vec{\rho},\tau_f} \min_{1\le i\le N} r_i \tag{2}$$

From this solution, the optimum association ($\mathcal{B}^*$) can be derived as follows. A user in range of an FBS operating at its computed power level will be associated with that FBS. All other users will be allocated to the MBS.

In the optimum solution, as the FBSs will equally divide the τ_f among its users, the FBS associated with the maximum number of users (bottleneck FBS) will serve the lowest data rate. As the users served by the bottleneck FBS and the users served by the MBS occupy different time slots, the optimum allocation must provide equal rate to all such users. Recall that $\mu(j,\rho(j))$ is the number of users in the coverage range of FBS j operating at power level $\rho(j)$. Thus, the total number of users served by the MBS ($N - \sum_{j=1}^{M} \mu(j,\rho(j))$) and the maximum number of users among the FBSs ($\max_{j\in[1,M]}\{\mu(j,\rho(j))\}$) will together determine the allocation. Note that all these users will be served in different tiles and so, their minimum fractional rate will be $r_i = 1/(N-\sum_{j=1}^{M}\mu(j,\rho(j))+\max_{j\in[1,M]}\mu(j,\rho(j)))$. So the optimization objective can be rewritten as:

$$\max_{\vec{\rho}}\{\frac{1}{N-\sum_{j=1}^{M}\mu(j,\rho(j))+\max_{j\in[1,M]}\mu(j,\rho(j))}\} \tag{3}$$

$$= \max_{\vec{\rho}}\{\sum_{j=1}^{M}\mu(j,\rho(j)) - \max_{j\in[1,M]}\mu(j,\rho(j))\} \tag{4}$$

and τ_m^* and τ_f^* can be uniquely determined by

$$\tau_m^* = \frac{N-\sum_{j=1}^{M}\mu(j,\rho(j))}{N-\sum_{j=1}^{M}\mu(j,\rho(j))+\max_{j\in[1,M]}\mu(j,\rho^*(j))} \tag{5}$$

$$\tau_f^* = 1-\tau_m^* \tag{6}$$

After the simplifications, the resulting objective (Equation 4) has only one variable ($\vec{\rho}$) in the outer max operator, which makes it easier to design solutions.

An Example (Figure 2): Please be noticed that the transmission and interference ranges are shown as circular and identical in some examples of this work for simplicity of discussion. However, these assumptions are not required in our solutions. In Figure 2, each of the two femtocells has two power levels. The zero power level is not shown for simplicity as it leads to lower $maxmin$ rate than the other combinations shown in the figure. For each power combination the optimum τ_m and the corresponding rates for all users are shown. The (Hi, Lo) combination of power levels for the two femtocells leads to the optimum $maxmin$ rate vector $\langle\frac{1}{3},\frac{1}{3},\frac{1}{3},\frac{1}{3},\frac{1}{3}\rangle$. Here, $\sum_{j=1}^{M}\mu(j,\rho(j)) = 4$ and $\max_{j\in[1,M]}\mu(j,\rho(j)) = 2$. The argument of (4) is $4-2=2$. By using the expression for τ_m^*, we get $\tau_m^* = 1/3$. The macrocell is serving 1 user (E) which gets a rate of 1/3. As $\tau_f^* = 2/3$, and both femtocells are serving two users each, all users are assigned a rate of 1/3.

Theorem 4.1: The $maxmin$ rate allocation problem P1 is NP-hard.

Proof: Please refer to our supplemental material for proof. ■

B. Centralized Resource Allocation (NINT)

A central server periodically collects topology information from all the users, computes the optimal solution and informs the FBSs and the users. A discussion of constructing conflict graphs is presented in section VII, and overhead messages are described and counted in the simulation section. Observe that if the maximum weight FBS is known in an optimal solution, i.e., the $\max_{j\in[1,M]}\mu(j,\rho(j))$ term is known in formulation (4), we can then solve the problem by solving an instance of the MWIS (maximum weight independent set) problem. We will explore all possible values of that term to arrive at the optimum solution. Our approach is to first model the constraints using a conflict graph and then solve multiple instances of the resulting MWIS problems (Algorithm 1).

First we create the conflict graph for the FBSs considering the various power levels. A node is created for each combination of power level and FBS ID. The *weight* of this node is counted by the number of users within the transmission range of the FBS at the chosen power level. Of course, some extra information needs to be stored for this node,

such as FBS ID, location, power level, and the weight. If the transmission range of one node, i.e., the transmission range of this FBS at corresponding power level, overlaps with the interference range of another node, an edge is added between two such nodes. Observe that nodes corresponding to the same femtocell, but for different power levels, will form a clique. As the topology of the conflict graph depends only on power levels and locations of FBSs, we only need to update the weight of each node at runtime, thus the overhead is relatively low. Figure 3 shows the conflict graph for Figure 2.

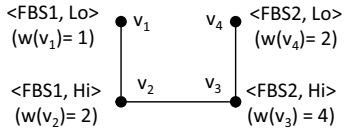

Fig. 3. Conflict Graph for scenario in Figure 2

Note that by substituting the nubmer of users with the summation of normalized weight of users, this model can be easily modified to work for the $weighted\ maxmin$ fairness problem.

The centralized resource allocation algorithm (Algorithm 1) uses the conflict graph to compute the power allocation ($\vec{\rho}$) for all FBSs based on (4). The variables Q and $nmax$ are used to keep track of the independent set and the maximum weight of femtocells in that independent set, respectively (Lines 3-4). Set S is an enumeration of weights of all nodes (Line 5). Next, the independent set of nodes that maximize expression (4) is computed by trying all possible values of the second term in (4) (Lines 6-15). In each iteration, the variable s takes on values from the set S. Only the nodes with weight at most s is considered for constructing the induced subgraph G'. With a slight overuse of the term w, we use $w(I)$ to indicate the total weight of all nodes in the set I. For this induced subgraph the max weight independent set is computed, and stored if it is the best thus far. The optimum independent set is then used to compute the power allocation (Lines 16-22). Note that as shown in the previous section, using ρ^*, τ_f^* and $\mathcal{B}^*$ can be computed.

This algorithm gives the optimum solution to the $maxmin$ problem if the MWIS can be exactly computed. However, MWIS is a NP-hard problem [45]. We can use a polynomial time approximation approach for the MWIS problem in line 10 . For example, a greedy algorithm that finds a maximal independent set can be used, which has a complexity of $O(M^2)$. Then from line $8, 9, 10$, the complexity of algorithm 1 can be denoted by $M * (M + M^2 + O(M^2))$, which is $O(M^3)$.

Regardless which algorithm we use for the MWIS problem in line 10, we can always achieve a bound of $max\{\beta, 1/N\}$, where β is the fraction of users (among all users) that are not covered by any femtocell, and N is the total number of users.

Theorem 4.2: If βN users are outside the range of any femtocells, where $0 \leq \beta \leq 1$, and an approximation algorithm is used for the MWIS subproblem in Algorithm 1, then the lowest rate allocated by this algorithm will be at least $max\{\beta, 1/N\}$ times the lowest rate in the optimum rate allocation.

Algorithm 1: Centralized Resource Allocation (NINT)

```
1  input: conflict graph G
2  output: ρ⃗: power allocation vector for FBSs
3  Q ← Φ // maximum independent set
4  nmax ← 0 // maximum weight of FBSs from Q
5  S ← set of possible values for the #users in a femtocell
6  foreach s in S do
7      create an empty graph G'
8      V(G') ← {v|v ∈ V(G) s.t. w(v) ≤ s}
9      E(G') ← edges induced by V(G') in G
10     I ← max weight independent set of G'
11     if w(I) − s > w(Q) − nmax then
12         Q ← I
13         nmax ← s
14     end
15 end
16 for j ∈ (1..M) do
17     if ∃q ∈ Q s.t. id(q) = j then
18         ρ(j) ← level(q) //set this FBS the stored power level
           of node q.
19     else
20         ρ(j) ← 0
21     end
22 end
```

Proof: Let the value of $\sum_{j=1}^{M} \mu(j, \rho(j))$ be A^{opt}, and the value of $\max_{j\in[1,M]} \mu(j, \rho(j))$ be B^{opt} in the optimum solution. Then the minimum rate allocated by the optimum solution to any user will be $r^{opt} = \frac{1}{N - A^{opt} + B^{opt}}$. Since algorithm 1 tries all possible values of $\max_{j\in[1,M]} \mu(j, \rho(j))$. When it uses the value of B^{opt} as largest(s in Line 6 of Algorithm 1), let the computed value of $\sum_{j\in[1,M]} \mu(j, \rho(j))$ ($w(I)$ in Lines 10-11) be A. So, the minimum throughput computed by our algorithm is $r \geq \frac{1}{N - A + B^{opt}}$. So,

$$\frac{r}{r^{opt}} \geq \frac{N - A^{opt} + B^{opt}}{N - A + B^{opt}} > \frac{N - A^{opt}}{N - A} > \frac{N - A^{opt}}{N} \tag{7}$$

As $A^{opt} \leq (1 - \beta)N$, we have,

$$\frac{r}{r^{opt}} > \frac{N - (1 - \beta)N}{N} = \beta \tag{8}$$

On the other hand,

$$\frac{r}{r^{opt}} \geq \frac{N - A^{opt} + B^{opt}}{N - A + B^{opt}} \geq \frac{B^{opt}}{N - A + B^{opt}} \geq \frac{B^{opt}}{N} \geq \frac{1}{N} \tag{9}$$

Therefore, the algorithm is bounded by $max\{\beta, 1/N\}$. ■

C. Distributed Approach (NINT)

In the distributed algorithm (Algorithm 2) each FBS attempts to increase or decrease its power level and evaluate its impact within the local neighborhood to determine the best action to take. We assume the cost of exchanging messages among neighboring femtocells is negligible by using the broadband backbone. The impact is evaluated by the change to the argument of Formula (4). If some users have left the FBS,

then the FBS attempts to increase its power level (Lines 3-11). It needs to obtain updated information on the number of users that can be supported if a higher power level is used by FBS j (Lines 5-7). Then the best power level is selected based on the argument to (4). If the number of users currently being served is the highest in the neighborhood then reducing it could possibly lead to increase in the argument to (4). For such a scenario, all power levels lower than the current one is explored in consultation with the interfering neighbors and the best power level is then selected (Lines 12-19).

Algorithm 2: Distributed Resource Allocation (NINT) at FBS f_j

```
1  input: power level ρ(j); number of users μ(j, ρ(j)); current
     ρ(m) and μ(m, ρ(m)) for each interfering neighbor m.;
2  output: power level ρ(j) ;
3  if some user(s) have left the femtocell then
4      foreach power level k higher than the current do
5          foreach interfering FBS f_m do
6              obtain μ(m, ρ(m)) from f_m for highest feasible ρ
                 if f_j switches to level k
7          end
8          compute adjustment to arg of (4)
9      end
10     select power level with max increase to arg (4)
11 end
12 if μ(j, ρ(j)) is the highest in the neighborhood then
13     foreach power level k smaller than the current do
14         foreach interfering FBS f_m do
15             obtain μ(m, ρ(m)) from f_m for highest feasible ρ
                 if f_j switches to level k
16         end
17         compute adjustment to arg of (4)
18     end
19     select power level with max increase to arg (4)
20 end
```

V. Resource Allocation with Interfering Femto-Cells

A. The Interfering Model

Allowing for interfering femtocells in the solution can lead to higher throughput. Consider the scenario of Figure 4(a), if we apply the NINT model, then in one of the optimum solutions, FBS1 will be selected and the power level for FBS2 will be set to 0. As a result the optimum value of τ_f is $2/3$, and the corresponding rate vector is $\langle 1/3, 1/3, 1/3\rangle$. However, if we allow for interference, then τ_f can be set to 1 (i.e, macrocell is not active), and FBS1 can transmit to A and FBS2 can transmit to C simultaneously for half of the tiles. In the remaining half, FBS1 can transmit to B, thus resulting in a rate vector $\langle 1/2, 1/2, 1/2\rangle$.

This kind of scheduling problem can be solved by constructing a conflict graph of links (we call it link-conflict graph or LCG to avoid confusion) and by performing a node coloring of this graph. However, our problem is quite different from prior work on scheduling flows in ad-hoc networks [33], [35] as it involves power assignment, and a macro base-station.

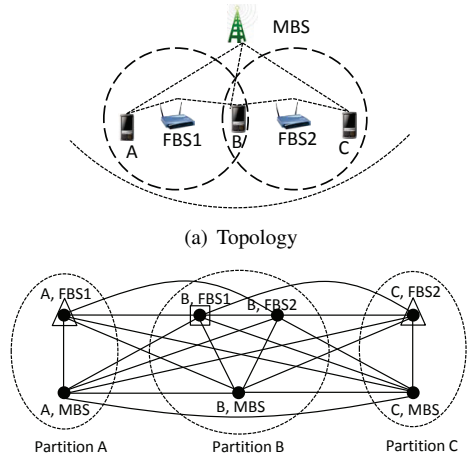

(a) Topology

(b) LCG and Partition Coloring Problem

Fig. 4. Operating Femtocells under interference (a) Two interfering femtocells (b) The link-conflict graph colored with two colors (triangle and square).

Each node in the LCG represents a communication link. If an FBS can communicate with a user at more than one power level, the miminum power level allowing the communication is selected. So, for a given user, there will be multiple nodes corresponding to links of various FBSs and the MBS. Such nodes corresponding to a single user will form one group, such that each group corresponds to exactly one user. The nodes in the LCG are thus partitioned into groups. All communication links that cannot be active simultaneously (due to interference or conflicting user occupancy), will be connected with edges in LCG. For example, nodes in the same group form a clique.

Constructing such kind of link conflict graph is outside the scope of this paper. We recommend to use techniques from [5] which can do the job within milliseconds. This procedure can be even faster considering that some users will stay in the same place within a short interval, thus only part of the graph needs to be updated on the fly.

Unlike the NINT model, the LCG based INT model allows a single FBS to transmit at different power levels to different users. Also, the allocation is more fine-grained as each tile is allocated to a specific user. Whereas in the NINT model, only the portions of tiles to macrocell and FBSs(τ_m,τ_f) are determined. *Suppose we color the graph with the least number of colors such that at least one node in each group is colored.* We name this problem as *partition coloring problem.* The colors represent tiles when the corresponding subset of links will be activated. Minimizing the colors is equivalent to minimizing the number of tiles needed to transmit one unit of data to each user node. If we focus on the optimal solutions that have repeated schedules and serve one user with exactly one tile within a schedule cycle, then we have maximized the minimum throughput by solving the partition coloring problem.

Definition 5.1: **Partition Coloring Problem:** Consider a graph $G = (V, E)$ with nodes partitioned into x groups

$g_1 \cdots g_x$. Compute a color assignment that assigns a color to exactly one node in each group, such that nodes with the same color do not share an edge, and the number of colors is minimized.

The partition coloring problem for the scenario in Figure 4(a) is shown in Figure 4(b). The triangles and the square represent two colors which correspond to two tiles in the optimum solution. By repeating this tile assignment for each pair of tiles, we can achieve the rate vector $\langle 1/2, 1/2, 1/2 \rangle$, for the three users. This also corresponds to the result discussed earlier in this section.

B. Centralized Algorithm (INT)

Algorithm 3 colors the partition graph by repeatedly picking up a maximal independent set and assigning the lowest color (or tile) to this set. After that, the partitions of all the nodes in the sets are removed from the partition graph (Lines $5-11$). After the coloring, it tries to reuse some colors on some nodes following the $maxmin$ metric (Line 12-19).

Observe that by controlling the elements of each independent set and the portion of colors assigned to each set, the $weighted\ maxmin$ fairness can also be addressed by the INT model.

Algorithm 3: Centralized Partition Coloring (INT)

1 **Input:** Graph $G(V, E)$ with N partitions denoted as $V_1 ... V_N$, $\bigcup_{i=1}^{N} V_i = V$
2 **Output:** Colored $V^C \subseteq V$ s.t. $V^C \cap V_i = 1$; $\forall i \in [1, N]$
3 $t \leftarrow 0$
4 $V^C \leftarrow \Phi$
5 **while** V *is not an empty set* **do**
6 $t \leftarrow t + 1$
7 Pick a maximal independent set $V^M \subseteq V$
8 Assign color t to all vertices $v \in V^M$.
9 Remove V_i from V, $\forall V_i \cap V^M \neq \Phi$, and remove all edges that have at least one end point in V_i
10 $V^C \leftarrow V^C \cup V^M$
11 **end**
12 **for** *color* $i \leftarrow 1$ *to* t **do**
13 Sort $v \in V^C$ in increasing order by # colors of v
14 **foreach** $v \in V^C$ **do**
15 **if** *None of* v *and its neighbors has been colored by* i **then**
16 Color v with i
17 **end**
18 **end**
19 **end**

Algorithm 3 takes at most $1 + \Delta$ colors to color G where Δ is the maximum degree of nodes in V without considering intra-partition edges. The proof for this assertion is similar to the proof for the bound on any greedy algorithm for proper vertex coloring [24]. Further, as partition coloring is a generalization of proper vertex coloring, therefore, it is not possible to design a polynomial time algorithm that guarantees coloring V in less than $1 + \Delta$ colors [24].

C. Localized Implementation (INT)

In this subsection, we propose an *incremental, localized* implementation for the coloring assignment problem, which can lower down the system overhead and insertion time of a new user. We follow our previous assumption in the NINT model that the cost of exchanging messages among neighboring femtocells is negligible by using the broadband backbone.

Let us call the nodes in link-conflict graph G that represent the links between FBS f_j and its users as *the nodes of* f_j. We define the local link-conflict graph G_L^j of f_j as a subgraph of G, which only involves the *nodes of* f_j and other nodes (edges) that conflict with (incident on) these nodes. When a new user comes to f_j, it will show up as a new partition in G_L^j.

Initially, the centralized algorithm will be called. Let t be the returned number of colors. The localized implementation (Algorithm 4) works as follows. Whenever a user moves away from the transmission range of its FBS, it randomly selects a *proxy FBS* at its new location, which will help the user in securing a new time slot. Let f_j be the *proxy FBS*. If some color $i \in [1, t]$ is available, i.e., assigning this color will not cause conflict in G_L^j, it will assign the color and return (Line $3-4$). If not, the local adjustment among neighborhood will be triggered by f_j. To that end, f_j and its neighbors will first free all their assigned colors (Line 6), this results in some partitions (users) previously served by these FBSs becoming uncolored. Then the same technique as in the centralized algorithm will be explored (Line 8), i.e., for each color $i \in [1, t]$, find a maximum independent set in the local conflict graph that can be colored by i. Color i is assigned to this set and the local link-conflict graph is updated. Finally, if this algorithm is not able to color all partitions in the neighborhood, then the centralized algorithm is called (Line 12).

Algorithm 4: Localized Coloring At proxy f_j

1 **Input:** Local Partition Graph of f_j, new user u
2 **Output:** A new schedule with all local partitions colored
3 **if** *Some color* $i \in [1, t]$ *can be assigned to the node corresponding to* (f_j,u) *in* G_L^j **then**
4 Color it with i
5 **else**
6 f_j and its neighbors free all assigned colors, flag corresponding partitions in their partition graphs as uncolored
7 **for** *color* i *from 1 to* t **do**
8 Exploit the same techniques as in centralized algorithm to color all uncolored local partitions
9 **end**
10 **end**
11 **if** *not all local partitions are colored* **then**
12 Call the centralized algorithm
13 **end**

VI. Simulations

We compare our solutions with two baseline algorithms and evaluate the minimum throughput, average throughput,

and the impact to throughput due to factors such as femtocell density, the arrival rate and speed of users.

A. Simulation Settings

Our simulations are conducted using the open source LTE-EPC Network Simulator (LENA) [48] derived from the ns-3 project. LENA implements a spectrum framework based on the LTE spectrum model as described in 3GPP TS36.101 [46], which allows the use of different spectrum models for different types of cells. Specifically, it uses an outdoor propagation model for macrocells and an indoor propagation model for femtocells. A trace-based Jakes fading model based on 3GPP TS36.104 [47] was also included. The typical parameters for the fading model were varied depending on the user's speed for both the pedestrian and vehicular scenarios as specified in Annex B.2 of 3GPP TS36.104. A square region of $800m \times 800m$ is considered in the simulation. A macrocell of height $20m$ is placed at the center of this region with a transmission range of $600m$ that allows full coverage of the area. Femtocells are deployed indoor at randomly chosen locations. The size of each building is $10m \times 10m$, and femtocells are placed at the center of those buildings on the ground. For each femtocell, 3 power levels were available (p_0, p_1 and p_2). p_0 is set to 0, while p_1 and p_2 result in transmission radii of $50m$ and $100m$, and interference radii of $80m$ and $150m$, respectively.

The default value of downlink bandwidth in our simulation is 26, i.e., resource block (RB) size is 26. In the LENA simulator, resource block group (RBG) is the minimum unit of resource to allocate. Based on the specifications in 3GPP TS36.213 table 7.1.6.1-1, a downlink bandwidth of 26 results in $26/2 = 13$ RGBs in each subframe. The resource allocation algorithms are implemented in the MAC layer, and downlink RBGs are allocated to femtocells based on those algorithms. Mobile users arrive at this network at various arrival rates (with i.i.d. inter-arrival time) and speeds, and do a random walk for $60s$. Saturated UDP traffic over downlink is generated for every user in the simulation. During their connection time, users report their topology information to base stations using an uplink channel. The duration of the simulation for every scenario was chosen to be 180 seconds.

To evaluate the performance of our solutions in different environments, we vary the values of femtocells, arrival rates and speeds of users to generate multiple scenarios. Number of femtocells is selected from $\{10, 20, 30, 40, 50,$ and $60\}$, arrival rates of users from $\{10, 20, 30, 40, 50, 60$ users/min$\}$. Speeds of users are also varied within $\{3.6\ km/h$ (pedestrian), $10, 20, 30, 40, 50, 60\ \ km/h$ (vehicular)$\}$. Unless otherwise specified, the default settings are, 30 FBSs, 30 $users/min$ arrival rate and 3.6 km/h of moving speed.

We use the DRA+ algorithm proposed in [43] as our baseline algorithm, which schedules interfering neighboring femtocells via distributed hashing. As DRA+ does not consider power adjustment, we implement one instance of DRA+ for each power level:

DRA-P1 implements DRA+ algorithm on femtocells, assuming all femtocells work at power level p_1.

DRA-P2 implements DRA+ algorithm on femtocells, assuming all femtocells work at power level p_2.

B. Simulation Results

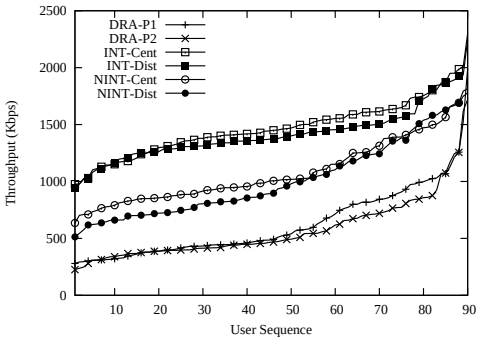

Fig. 5. Users are sorted by their throughputs. One point is plotted on the line for every 3 users.

Lexicographic Throughput: Figure 5 shows the performance of the six algorithms evaluated for a single scenario with default settings. Users are sorted by the amount of data received during $60s$ of random walk. It shows that DRA-P1 performs better than DRA-P2. This is expected since the interfering neighbors are fewer when femtocells work at power level p_1 than at p_2. Our distributed solutions perform close to the centralized algorithms under both non-interfering and interfering models. *Compared to the baseline algorithms, while the non-interfering model achieves more than $2x$ of the minimum throughput, the interfering model achieves more than $3x$ of the minimum throughput.* Those improvements are expected because the DRA+ algorithm allocates resources on a per-femtocell basis (not per-user basis), without considering the power assignments of femtocells and densities of users, which are well exploited in our algorithms.

Algorithm Comparison: Figure 6 shows the comparison of pairs of algorithms using scatter plots of users, which leads to similar conclusions as above.

Impact on Throughput due to Various Factors: Next, we evaluate the impact on throughput by varying the number of femtocells, arrival rates and speeds of users. For this, we keep two factors as constant, and evaluate the impact of the third factor. Each data point shown is an average of 5 scenarios, where every scenario has a random placement of femtocells.

Figure 7 (a) shows *when the number of femtocells increases, the minimum throughput among all users and scenarios tends to increase in our algorithms*. Note that when the number of femtocells is more than 50, the minimum throughput in the INT model starts to decrease, due to the fact that although pair-wise interference between active links has been addressed in this model, *the accumulated interference becomes high enough at this point to affect the throughput. DRA algorithms, on the other hand, do not benefit as much when increasing the density of femtocells. DRA-P2 is better*

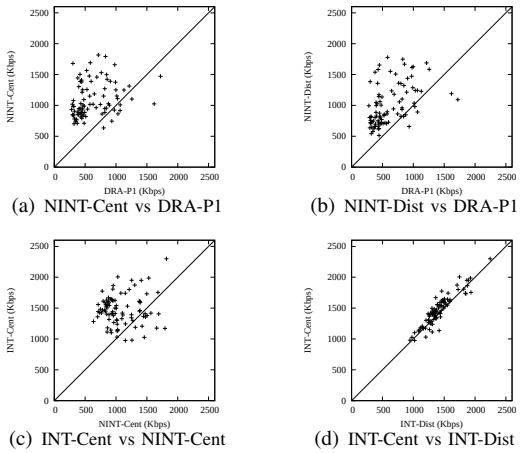

(a) NINT-Cent vs DRA-P1 (b) NINT-Dist vs DRA-P1

(c) INT-Cent vs NINT-Cent (d) INT-Cent vs INT-Dist

Fig. 6. Scatter plots of throughputs of 90 users, one point denotes one user

than DRA-P1 only when the number of femtocells is small (10 femtocells). This can be explained by the fact that DRA algorithms do not perform power adjustment, and spectrum resource is divided equally among the neighboring femtocells. When the number of interfering neighbors is small in sparse deployments, DRA-P2 performs better due to its larger coverage area. However, when the number of interfering neighbors becomes large in dense deployments, the resource allocated to each femtocell starts to drop significantly, resulting in lower throughput to users in both algorithms. *Overall, the NINT and INT models can achieve up to* $2x$ *and* $3x$ *of the minimum throughput.* Average throughput in the same set of scenarios is shown in Figure 7 (d), which shows similar trends. Similarly, Figures 7 (b) and (e) show that *minimum and average throughputs drop when the arrival rate increases (more users in the system)*, and Figures 7 (c) and (f) show that *the minimum throughput increases slightly, and the average throughput decreases slightly when the speed of users is increased from* $10km/h$ *to* $60km/h$. This is because when the speeds of users is increased, the chance that a user sees a femtocell in its lifetime increases. Thus the user that receives the lowest throughput has higher chances to increase its throughput. However, due to the Doppler effect, system-wide throughput gain is offset by the increased speed.

Approximation Ratio of INT Model: To understand the gap between our INT algorithm and its optimal solution, we then formulate the Partition Coloring problems as an Integer Linear Programming problem, and use lp_solve [32] to obtain the optimal solution. The partition graphs are re-constructed from the log files of our previous simulations, which guarantees that this evaluation is based on realistic settings. We show the resulting average number of colors by partitions for each algorithm. Note that the number of partitions (users) shown in Figure 8 are counted only for femtocell users, since any of the macrocell partitions (users) would have conflicting links with all other partitions (users) and will take one color in any algorithm.

From Figure 8, it is clear that performance of our INT-Cent algorithm is very close to the optimal, even though the approximation ratio tends to decrease in larger graphs (i.e., more femtocell users).

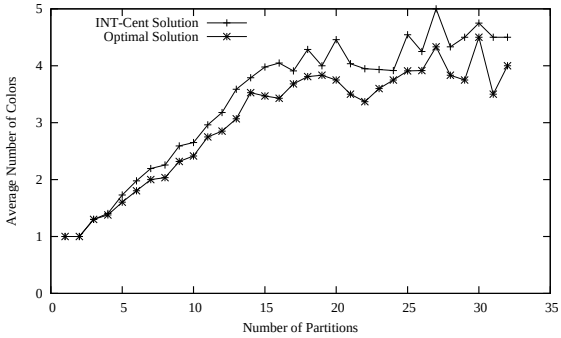

Fig. 8. Average number of colors needed by INT-Cent algorithm and the optimal to color the same partition graph.

System Overhead: In simulations, in order to create the conflict graph, whenever a change in the topology occurs, users send their topology information to base stations through an uplink channel. Next, we evaluate the overhead of acquiring and sending this information. For the NINT model, we assume femtocells periodically send becaons at different power levels, and a node needs to send a message of 2 bytes for each beacon it receives, indicating which femtocell/powerlevel the beacon is from. For the INT model, we assume that a message of 2 bytes needs to be sent by a node for each pair of conflicting links it finds (assume there is some throughput test mechanism to identify conflicting links).

Figure 9 (a) shows the overhead imposed by those control packets as a percentage of all data packets with different numbers of femtocells in the network. Note that we did not count the coordination packets sent between neighboring FBSs in the distributed solutions, since their cost is relatively low. It shows that in all algorithms when users walk at $3.6km/h$, the percentage of overhead increases with increase in the number of femtocells, due to increase in the number of interference sources. While the INT-Cent algorithm has the highest overhead, *the distributed solutions can save upto* $1/3^{rd}$ *of system overhead from their centralized counterparts*. Recall from Figure 7 (d) that the total throughput of the network is also increasing when more femtocells are deployed, implying that the total number of overhead packets is increasing at a higher rate. Figure 9 (b) shows that given the same set of femtocells and users, when the speed of users is increased from $10km/h$ to $60km/h$, the percentage of overhead increases at an even higher rate. This is caused by both the increasing chance of seeing interfering femtocells, and the result of fast fading channels. However, the savings of overhead in the distributed solutions compared with the centralized solutions are still substantial.

VII. Discussion and Future Work

- **Construct Conflict Graphs** This paper takes conflict graphs as the inputs of our algorithms. However, con-

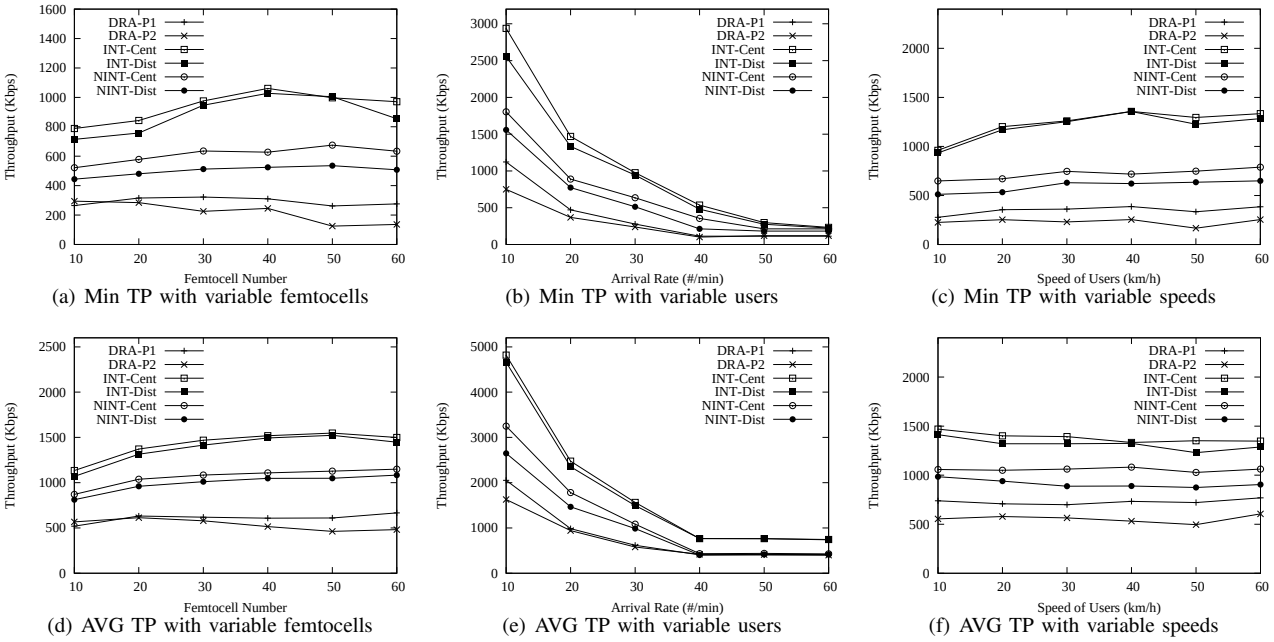

(a) Min TP with variable femtocells (b) Min TP with variable users (c) Min TP with variable speeds

(d) AVG TP with variable femtocells (e) AVG TP with variable users (f) AVG TP with variable speeds

Fig. 7. Variation of minimum/average throughput of all users due to various factors. (a,d) Minimum/Average throughput increases as #femtocells increases (arrival rate $= 30/min$, speed $= 3.6km/h$). (b,e) Minimum/Average throughput decreases as the arrival rate of users increases (#femtocells $= 30$, speed $= 3.6km/h$). (c,f) Minimum/Average throughput increases/decreases as the speed of users increases (#femtocells $= 30$, arrival rate $= 30/min$).

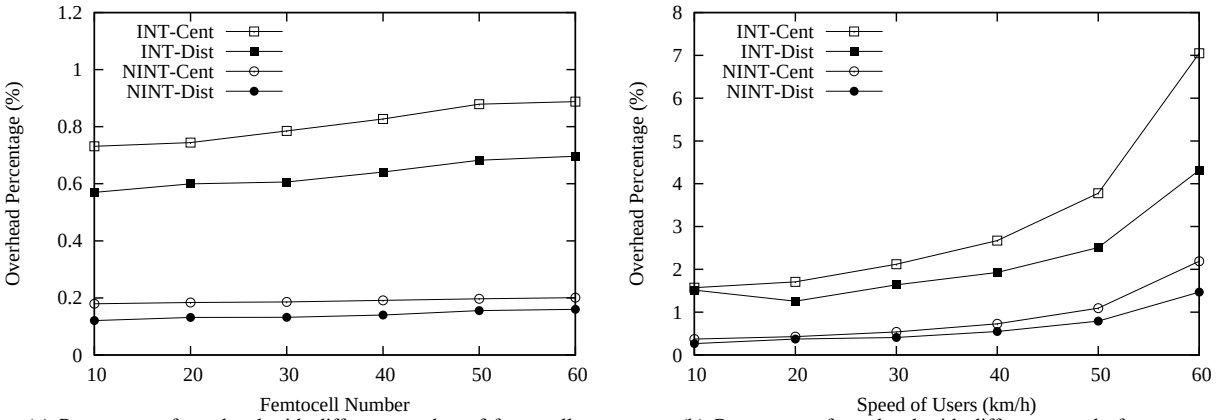

(a) Percentage of overhead with different number of femtocells (b) Percentage of overhead with different speed of users

Fig. 9. Percentage of overhead with different number of femtocells and mobile speeds (a) Percentage of overhead slowly increases as the network becomes denser (arrival rate = 30/min, speed = $3.6km/h$). (b) Percentage of overhead increases faster when increasing the speed of users (#femtocells = 30, arrival rate = 30/min).

structing such kind of conflict graphs sometimes could be nontrivial. Although conflict graphs are constructed based on the knowledge of users' locations in our simulations, this approach might be neither accurate nor feasible due to the lack of knowledge of users' locations. However, we can construct the conflict graphs without knowing users' locations.

Constructing conflict graph for the NINT model is relatively simple. Recall that the conflict graph in NINT model is stable, i.e., it does not need to be reconstructed from time to time. For any FBS, it only needs to figure out which neighbor (at what power level) it interferes with, for once. This kind of requisite is very similar to the one in [43], in which every FBS needs to find out its set of interfering neighbors. To obtain such conflict graph, one way is to let each FBS send out beacons at different power levels, and look at the received signal strength of pilots from others. The second way is to construct the conflict graph based on users' reports. Whenever a user associated with some FBS encounters interference, it reports to the FBS. Then by testing the throughputs (also called bandwidth test) with and without the presence of another neighbor, this FBS can figure out if it interferes with the FBS (at the current power level) or not.

In NINT model, other than the conflict graph of femtocells, we also need to know the weight (# of users) of FBSs at each power level. This weight info need to be updated from time to time. Similar to the above mentioned method, by letting FBSs send beacons at different power levels, users can report their received signal strengths from each FBS in vicinity. In this way, FBSs know how many users are available to serve at each power level.

Unlike the NINT model, the link conflict graph in INT model is more complicated and needs to be updated on runtime. Most prior research on conflict graph construction uses bandwidth tests that tests a pair of links based on the observations of throughputs with presence and absence of simultaneous transmissions [21], [38]. This approach is also adopted in a latest femtocell resource allocation work [8]. In this work, we also assume that a bandwidth test framework is sufficient to construct the link conflict graph, and we evaluated the overhead of such approach in our simulation part.

Other than bandwidth test, another online approach is proposed in [5] which can do the job within milliseconds as claimed in the work. However, this approach requires to modify the air interface, which is usually prohibitive in cellular network. If this approach could be applied to femtocell network, the procedure of constructing link conflict graph might be even faster considering that some users will stay in the same place within a short interval, thus only part of the graph needs to be updated on the fly.

- **SINR based Interference Model** We have so far only considered binary interference model. Alternatively, the SINR model can be considered. In the SINR model, let $SINR(i,l)$ be the SINR at user i in tile l, then it must be larger than a threshold γ for successful reception in tile l. In some sense, our binary approach is only an approximation of the underlying SINR based model. Observe that $SINR(i,l)$ is dependent on the allocation of tile l on other femtocells, achieving $maxmin$ resource allocation and maximal throughput under SINR model will be more interesting and challenging.

  In order to solve this problem, we will explore a simplifying technique that limits the summation of noise only to neighboring femtocells by relaxing γ to $\gamma + \eta$, where η is appropriately chosen so that it bounds the maximum interference from all other non-neighboring femtocells. This construction will allow to focus on a limited number of neighboring femtocells for the purpose of scheduling and power assignment.

VIII. Conclusion

To address the $maxmin$ and $weighted\ maxmin$ problems in the context of resource allocation in femtocells, two models are considered in this paper. The non-interfering model selects an independent set of femtocells, and determines the resource allocation factors based on this set. For the interfering model, the problem is transformed into the partition coloring problem. Algorithms with provable bounds are designed for both models. Improvements of up to 3x is observed for the minimum throughput for the interfering model over previous work.

References

[1] Taking Wireless to the Max. *Business Week*, pages 101–102, November 2008.

[2] 3GPP. LTE HomePage. http://www.3gpp.org/article/lte.

[3] 3GPP. 3G Home Node B (HNB) Study Item Technical Report (Release 8). *TR 25.820 V8.2.0(2008-9)*, 2008.

[4] A. Agustin, J. Vidal, and O. Munoz. Interference Pricing for Self-organisation in OFDMA Femtocell Networks. *in European Workshop on Broadband Femtocell Networks - Future Network and Mobile Summit (FuNeMS)*, 2011.

[5] N. Ahmed, U. Ismail, S. Keshav, and K. Papagiannaki. Online Estimation of RF Interference. *in Proceedings of the 2008 ACM CoNEXT Conference*, 2008.

[6] M. Arslan, K. Sundaresan, S. Krishnamurthy, and S. Rangarajan. Design and Implementation of an Integrated Beamformer and Uplink Scheduler for OFDMA Femtocells. *MobiHoc*, 2012.

[7] M. Arslan, J. Yoon, K. Sundaresan, and S. Banerjee. Experimental Characterization of Interference in OFDMA Femtocell Networks. *in Proc. IEEE Infocom*, 2012.

[8] M. Arslan, J. Yoon, K. Sundaresan, S.V. Krishnamurthy, and S. Banerjee. FERMI: A Femtocell Resource Management System for Interference Mitigation in OFDMA Networks. *in Proceedings of the ACM MobiCom*, 2011.

[9] ATT. 3G Microcell. http://www.wireless.att.com/learn/why/3gmicrocell/.

[10] Y. Bejerano, S. Han, and L. Li. Fairness and Load Balancing in Wireless LANs using Association Control. *in Proceedings of the ACM MobiCom*, 2004.

[11] V. Chandrasekhar and J. Andrews. Uplink Capacity and Interference Avoidance for Two-tier Femtocell Networks. *Global Telecommunications Conference, 2007*, pages 3322–3326, 2007.

[12] V. Chandrasekhar and J. Andrews. Femtocell networks: A survey. *IEEE Communication Magazine*, 46(9):59–67, 2008.

[13] R.Y. Chang, Z. Tao, J. Zhang, and J. Kuo. A Graph Approach to Dynamic Fractional Frequency Reuse (FFR) in Multi-Cell OFDMA Networks. *in IEEE International Conference on Communications (ICC)*, 2009.

[14] H. Claussen. Performance of Macro- and Co-channel Femtocells in a Hierarchical Cell Structure. *in IEEE PIMRC*, Sep. 2007.

[15] W.H.L. David, S.W. Hui, and V.K.N. Lau. Cross-Layer Design for OFDMA Wireless Systems with Heterogeneous Delay Requirements. *in IEEE Trans. Wireless Comm.*, 6(8):2872–2880, 2007.

[16] WiMax.com FAQ. http://www.wimax.com/education/faq/.

[17] Femtoforum. Interference Management in UMTS Femtocells. http://www.femto forum.org/, 2008.

[18] Femtoforum. Femtocell Market Status Issue 1. http://www.femto forum.org/, 2009.

[19] A. Hatoum, N. Aitsaadi, R. Langar, R. Boutaba, and G. Pujolle. FCRA: Femtocell Cluster-based Resource Allocation Scheme for OFDMA Networks. *IEEE ICC 2011*, 2011.

[20] L. Ho and H. Claussen. Effects of User-deployed, Co-channel Femtocells on the Call Drop Probability in a Residential Scenario. *in IEEE PIMRC*, September 2007.

[21] V. Padmanabhan L. Qiu A. Rao J. Padhye, S. Agarwal and B. Zill. Estimation of Link Interference in Static Multi-hop Wireless Networks. In *in IMC*, 2005.

[22] J. Jang and K.B. Lee. Transmit Power Adaptation for Multiuser OFDM Systems. *in IEEE J. Selected Areas in Comm*, 21(2):171–178, 2003.

[23] M. Kaneko, P. Popovski, and J. Dahl. Proportional Fairness in Multi-Carrier System with Multi-Slot Frames: Upper Bound and User Multiplexing Algorithms. *in IEEE Transactions on Wireless Communications*, 7(1):22–26, 2005.

[24] M. Kubale. *Graph Colorings*. American Mathematical Society, 2004.

[25] G. Li and R. Simha. The Partition Coloring Problem and its Application to Wavelength Routing and Assignment. *in Proceedings of the First Workshop on Optical Networks*, 2000.

[26] L. Li, M. Pal, and Y. Yang. Proportional Fairness in Multi-rate Wireless LANs. *in Proceedings of the IEEE InfoCom*, 2008.

[27] J. Liu, Q. Chen, and H. D. Sherali. Algorithm Design for Femtocell Base Station Placement in Commercial Building Environments. *in Proc. IEEE Infocom*, 2012.

[28] J. Liu and C. Lin. Achieving Efficiency Channel Utilization and Weighted Fairness in IEEE 802.11 WLANs with a p-persistent Enhanced DCF. *MSN*, 2007.

[29] Y. Liu, M. Tao, B. Li, and H. Shen. Optimization Framework and Graph-Based Approach for Relay-Assisted Bidirectional OFDMA Cellular Networks. *in IEEE Transactions on Wireless Communications*, 9(11):3490–3500, 2010.

[30] D. Lopez-perez, A. Ladanyi, A. Jttner, and J. Zhang. OFDMA femtocells: A Self-Organizing Approach for Frequency Assignment. *in IEEE PIMRC*, 2009.

[31] D. Lopez-perez, A. Valcarce, G. De La Roche, and J. Zhang. OFDMA Femtocells: A Roadmap on Interference Avoidance. *IEEE Communications Magazine*, 47(9):41–48, September 2009.

[32] lp_solve. lp_solve 5.2.2.0. http://lpsolve.sourceforge.net/5.5/.

[33] H. Luo, S. Lu, and V. Bharghavan. A New Model for Packet Scheduling in Multihop Wireless networks. In *Proc. of ACM MOBICOM*, August 2000.

[34] H. Luo, X. Meng, R. Ramjee, P. Sinha, and L. (Erran) Li. The Design and Evaluation of Unified Cellular and Ad-Hoc Networks. *IEEE Transactions on Mobile Computing (TMC)*, 6(9):1060–1074, 2007.

[35] N. Vaidya and P. Bahl and S. Gupta. Distributed Fair Scheduling in a Wireless LAN. In *Proc. of ACM MOBICOM*, August 2000.

[36] S. Nanda. Teletraffic Models for Urban and Suburban Microcells: Cell Sizesand Handoff Rates. *IEEE Transactions on Vehicular Technology*, 42(4):673–682, November 1993.

[37] T.-D. Nguyen and Y. Han. A Proportional Fairness Algorithm with QoS Provision in Downlink OFDMA Systems. *in IEEE Comm. Letters*, 10(6):760–762, 2006.

[38] D. Niculescu. Interference Map for 802.11 Networks. In *in IMC*, 2007.

[39] Nokia Siemens Networks. LTE Performance for Initial Deployments. http://w3.nokiasiemensnetworks.com/NR/rdonlyres/ 4B75329B-3750-4BBB-8320-7113613AAB64/0/LTE-measurement-A4-1302.pdf.

[40] M. E. Sahin, I. Guvenc, M. R. Jeong, and H. Arslan. Handling CCI and ICI in OFDMA Femtocell Networks Through Frequency Scheduling. *IEEE Trans. Consumer Electronics*, 55(4):1936–1944, 2009.

[41] Z. Shen, J.G. Andrews, and B.L. Evans. Adaptive Resource Allocation in Multiuser OFDM Systems with Proportional Rate Constraints. *in IEEE Transactions on Wireless Communications*, 4(6):2726–2737, 2005.

[42] Spring. Spring Airave. http://www.nextel.com/en/services/airave/index-.shtml.

[43] K. Sundaresan and S. Rangarajan. Efficient Resource Management in OFDMA Femto Cells. *in ACM MOBIHOC*, May 2009.

[44] K. Sundaresan and S. Rangarajan. Adaptive Resource Scheduling in Wireless OFDMA Relay Network. *in Proc. IEEE Infocom*, 2012.

[45] Luca Trevisan. Inapproximability of Combinatorial Optimization Problems. *Technical Report TR04-065, Electronic Colloquium on Computational Complexity*, 2004.

[46] 3GPP TS36.101. E-UTRA User Equipment Radio Transmission and Reception. http://www.3gpp.org/ftp/Specs/html-info/36-series.htm.

[47] 3GPP TS36.104. E-UTRA Base Station Radio Transmission and Reception. http://www.3gpp.org/ftp/Specs/html-info/36-series.htm.

[48] Ubiquisys and CTTC. LTE-EPC Network Simulator. http://iptechwiki.cttc.es/LTE-EPC_Network_Simulator_(LENA).

[49] A. Valcarce, D. Lopez-perez, G. De La Roche, and J. Zhang. Limited Access to OFDMA femtocells. *in IEEE PIMRC*, 2009.

[50] Verizon. Network Extender. http://wirelesssupport.verizon.com/information/networkextender.html?t=2.

[51] P. Xia, V. Chandrasekhar, and J. G. Andrews. Femtocell Access Control in the TDMA/OFDMA Uplink. *in Proc. IEEE Global Telecommunications Conference*, 2010.

[52] R. Xie, F. R. Yu, and H. Ji. Energy-Efficient Spectrum Sharing and Power Allocation in Cognitive Radio Femtocell Networks. *in Proc. IEEE Infocom*, 2012.

[53] K. L. Yeung and S. Nanda. Channel Management in Microcell/Macrocell Cellular Radio Systems. *IEEE Transactions on Vehicular Technology*, 45(4):601–602, November 1996.

[54] Ji-Hoon Yun and Kang G. Shin. CTRL: A Self-organizing Femtocell Management Architecture for Co-channel Deployment. *in Proceedings of the ACM MobiCom*, 2010.

[55] A.N. Zaki and A. O. Fapojuwo. Optimal and Efficient Graph-Based Resource Allocation Algorithms for Multiservice Frame-Based OFDMA Networks. *in IEEE International Conference on Communications (ICC)*, 2009.

[56] Y.J. Zhang. A Multi-Server Scheduling Framework for Resource Allocation in Wireless Multi-Carrier Networks. *in IEEE Trans. Wireless Comm.*, 6(11):3884–3891, 2007.

[57] Y.J. Zhang and K.B. Letaief. Cross-Layer Adaptive Resource Management for Wireless Packet Networks with OFDM Signaling. *in IEEE Trans. Wireless Comm.*, 5(11):3244–3254, 2006.

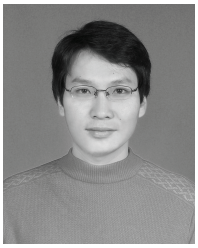

Zhixue Lu received his BS degree in Information Management and Information System from Peking University, China in 2005, and MS degree in Computer Science from Peking University, China in 2008. He is currently a PhD student at The Ohio State University, Columbus. His research interests include Femtocell Network, Dynamic Spectrum Access, and Game Theory.

Tarun Bansal received the BS degree in Computer Science and Engineering from Indian Institute of Technology, Roorkee, India, in 2006 and the MS degree in Computer Science from University of Texas at Dallas, Richardson, in 2009. He is currently a PhD student at Ohio State University, Columbus. His research interests include Cognitive Radio Networks, Dynamic Spectrum Access,and wireless spectrum resource allocation/management.

Prasun Sinha received his PhD from University of Illinois, Urbana-Champaign in 2001, MS from Michigan State University in 1997, and B. Tech. from IIT Delhi in 1995. Currently he is an Associate Professor in the Department of Computer Science and Engineering at Ohio State University. From 2001 to 2003, he was a Member of Technical Staff at Bell Labs, in Holmdel, New Jersey. His research focuses on ubiquitous networking. He has served as TPC co-chair for IWQoS 2011, TPC chair for ICST QShine 2009 and as TPC co-chair for IEEE BROADNETS 2010. He has won several awards including Lumley Research Award (OSU, 2009), CAREER award (NSF, 2006) Ray Ozzie Fellowship (UIUC, 2000), Mavis Memorial Scholarship (UIUC, 1999), and Distinguished Academic Achievement Award (MSU, 1997).

APPENDIX

In this part, We prove Theorem 4.1, which says the $maxmin$ rate allocation problem P1 is NP-hard.

Proof: We reduce the Maximum Independent Set problem for unit disks in a plane (MIS-DISKS), which is known to be NP-hard [1], to P1. In MIS-DISKS, the objective is to select a maximum subset of non-overlapping disks.

Given an instance of the MIS-DISKS problem with M disks, we construct an instance of P1. Each disk corresponds to a femtocell with its femto-BS situated at the center of that disk. Each femtocell has two power levels, zero and unit power level, where the latter corresponds to a unit transmission range and unit interference range. An additional femtocell f is added that does not overlap with any other femtocell (See Figure 1). A macro-BS is added with a large enough coverage range that includes the covered regions of all the femtocells.

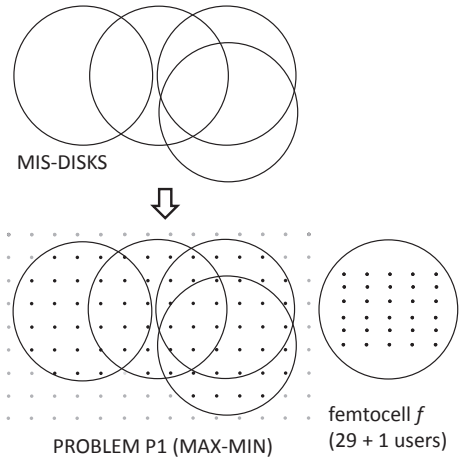

Fig. 1. Reduction for NP hardness. Here the radius of the circle is 3 times d, and $\eta(3)$ is known to be 29 [2]. So the additional femtocell f has 29+1 = 30 users. The dark dots represent the users. The gray dots are the lattice points outside the disks that were not selected to represent users.

Now consider a 2D lattice of points in the plane with a sufficiently high density (to be determined later). The lattice density will be chosen in such a way that the number of points within a unit disk is within a fixed range, say, $[K, K+\gamma]$, where $\gamma < \frac{K}{M}$. Each lattice point overlapping with any of the M femtocells will correspond to a user. In addition, $K+\gamma+1$ users are placed at any location within the range of femtocell f, thus making femtocell f the femtocell with the highest number of users.

If f is not in the optimum solution of the instance of P1, it can be added to increase the first term of expression Equation 4 with a lesser increase to the second term, leading to a resultant increase of the objective. So in the optimum solution to P1, f must be operating at unit power and the second term will have a value of $K+\gamma+1$.

Let S' be the set of disks corresponding to the femtocells other than f, that has a non-zero power allocation in the solution to P1. We claim that S' is a solution to the MIS problem. For the sake of contradition, let us assume that the optimum solution to the MIS problem, S, is such that $|S| > |S'|$. As the total number of users in range of the femtocells corresponding to S' is maximized, $K|S| \leq (K+\gamma)|S'|$. Therefore, $\gamma \geq \frac{|S|-|S'|}{|S'|}K \geq \frac{|S|-|S'|}{M}K \geq \frac{K}{M}$. But in our construction $\gamma < \frac{K}{M}$, which is a contradiction. Thus, $|S| \leq |S'|$, implying that S' is a solution to the MIS problem.

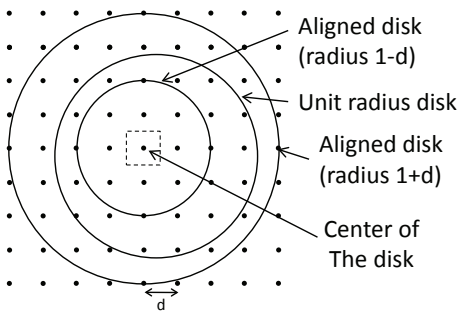

Fig. 2. Gauss's Circle Problem for Non-Lattice-disks: Alligned disks are lattice-disks. The square represents the region closest to the point at the center of the square.

Now we choose the appropriate value of lattice distance d ($d < 1$) such that the number of points within a unit disk is within the range $[K, K+\gamma]$. We say that a disk is a lattice-disk if its center coincides with a lattice point. If r is the ratio of the radius of the disk to the lattice distance, then using the Gauss' circle formula, the number of lattice points contained in it is represented as $\eta(r) = \pi r^2 + O(r)$ [2]. If the center of a unit disk is not aligned to a lattice point (Figure 2), then the number of lattice points will be within a range, $[K, K+\gamma]$. The nearest lattice point to any point on the plane is atmost at a distance of $\frac{d}{\sqrt{2}}$. So, centerd at that nearest lattice point, a lattice-disk of radius $1-d$ is fully contained within the unit disk, and a lattice-disk of radius $1+d$ will fully contain the unit disk. So the minimum number of lattice points for a unit disk, K will be atleast $\eta(\frac{1-d}{d})$, i.e., $K \geq \eta(\frac{1-d}{d}) = \pi(\frac{1}{d}-1)^2 + O(\frac{1}{d})$. Similarly, $K+\gamma$ will be atmost $\eta(\frac{1+d}{d})$, i.e., $K+\gamma \leq \eta(\frac{1+d}{d}) = \pi(\frac{1}{d}+1)^2 + O(\frac{1}{d})$. Therefore, $\gamma \leq \pi(\frac{1}{d}+1)^2 - \pi(\frac{1}{d}-1)^2 + O(\frac{1}{d}) = 4\pi(\frac{1}{d}) + O(\frac{1}{d})$. As $\frac{1}{d}$ increases, K grows quadratically but γ grows linearly. So for a sufficiently high value of $\frac{1}{d}$ (depends on M and the constants in $O(.)$), K will exceed γM, or, $\gamma < \frac{K}{M}$.

K and γ will both be polynomials in M. So, the total number of users created in this reduction is polynomial and the reduction is polynomial time, thus completing the proof. ■

REFERENCES

[1] B.N. Clark, C.J. Colbourn, and D.S. Johnson. Unit Disk Graphs. *Discrete Mathematics*, 86:165–177, 1990.

[2] G.H. Hardy. *Ramanujan: Twelve Lectures on Subjects Suggested by His Life and Work*. AMS Chelsea Publishing, New York, 3 edition, 1999.